螺纹接头处拉应力作用下的缝隙腐蚀行为

钟显康[1,2]，郑子奇[1]，莫林[3]，卿阳[4]，喻丝雨[1]，扈俊颖[1,2]

（1.西南石油大学 石油与天然气工程学院，成都 610500；2.油气藏地质及开发工程国家重点实验室，成都 610500；3.西南油气田公司天然气研究院，成都 610213；4.西南油气田川中油气矿，四川 遂宁 629000）

摘要：目的 研究N80钢在高温高压中缝隙和应力耦合作用下的腐蚀行为，为油井管的选材和螺纹选型提供参考。**方法** 以油管螺纹接头为研究对象，在高温高压釜模拟地层环境，采用电化学方法和表面分析技术，研究N80钢在缝隙单因素作用下和缝隙-应力耦合作用下的腐蚀行为。**结果** 仅有缝隙作用24 h后，缝内存在大量腐蚀产物堆积，缝外几乎没有腐蚀产物。40 ℃时的凹槽深度为17.2 μm，而70 ℃时的凹槽深度则达到82.7 μm。在缝隙和应力耦合作用24 h后，在缝隙口处发现有腐蚀产物堆积，缝隙内腐蚀程度比缝隙外腐蚀程度更为严重。40 ℃时，弹性形变试样的缝隙口处凹槽深度约为35.3 μm，塑性形变的试样缝隙口处凹槽深度约为41.3 μm；而70 ℃时，发生弹性变形和塑性变形的试样缝隙口处凹槽深度则分别为143.7 μm和243.9 μm。**结论** 缝隙和应力耦合作用使缝隙口处凹槽的深度加深，且深度随着腐蚀时间和温度的增加而增大，塑性形变时凹槽深度最大。这表明应力的施加会加剧N80钢的缝隙腐蚀，导致形成更深的腐蚀凹槽，这反过来又会导致应力的进一步集中，应力腐蚀风险增加。因此，缝隙和应力对N80钢在高温高压地层水环境中的腐蚀具有协同作用。

关键词：缝隙腐蚀；应力腐蚀；螺纹；高温高压

DOI：10.7643/ issn.1672-9242.2020.11.008

中图分类号：TG172 **文献标识码：**A

文章编号：1672-9242(2020)11-0052-08

Crevice Corrosion at Screwed Joint with Tensile Stress

ZHONG Xian-kang[1,2], *ZHENG Zi-qi*[1], *MO Lin*[3], *QING Yang*[4], *YU Si-yu*[1], *HU Jun-ying*[1,2]

(1. Petroleum Engineering School, Southwest Petroleum University, Chengdu 610500, China;
2. State Key Laboratory of Oil and Gas Reservoir Geology and Exploitation, Chengdu 610500, China;
3. Natural Gas Research Institute of Southwest Oil and Gas Field Company Chengdu 610213, China;
4. Central Sichuan Oil and Gas Deposit of Southwest Oil and Gas Field Company, Suining 629000, China)

ABSTRACT: The work aims to study the corrosion behavior of N80 steel under the combined crevice and tensile stress in high temperature and high pressure environment, to provide reference for selection of oil well pipe and thread. With screwed joint of oil tube as the research object, the corrosion behaviors of N80 steel under single factor and crevice-stress coupling factor were studied by electrochemical techniques and surface analysis methods in stratum simulated by high temperature and high pressure autoclave. Under the single action of crevice for 24 h, a large number of corrosion products accumulated in the crevice, and al-

收稿日期：2020-09-28；**修订日期：**2020-10-10

Received：2020-09-28；**Revised：**2020-10-10

作者简介：钟显康（1984—），男，博士，教授，主要研究方向为油气田腐蚀与防护。

Biography：ZHONG Xian-kang (1984—), Male, Doctor, Professor, Research focus: corrosion and protection in oil and gas.

通讯作者：扈俊颖（1982—），女，博士，副教授，主要研究方向为油气田腐蚀与防护。

Corresponding author：HU Jun-ying (1982—), Female, Doctor, Associate professor, Research focus: corrosion and protection in oil and gas.

most no corrosion products accumulated outside the crevice. The groove depth at 40 ℃ was 17.2 μm, while the groove depth at 70 ℃ was 82.7 μm. Under the combined effect of crevice and stress for 24 h, corrosion products were found to accumulate at the crevice mouth, and the corrosion degree in the crevice was more serious than that outside the crevice. At 40 ℃, the groove depth at the crevice mouth with elastic deformation specimen was about 35.3 μm, and that at the crevice mouth with plastic deformation specimen was about 41.3 μm. However, at 70 ℃, the groove depth at the crevice mouth of the specimen with elastic deformation and plastic deformation was 143.7 μm and 243.9 μm respectively. Under the coupling effect of crevice and stress, the depth of groove at the crevice mouth is deepened, and with the increase of corrosion time and temperature, the depth of groove increases to the deepest when plastic deformation occurs. This shows that the application of stress will aggravate the crevice corrosion of N80 steel and lead to the formation of deeper corrosion grooves, which in turn will lead to the further concentration of stress, resulting in higher stress corrosion. Therefore, crevice and stress have synergistic effect on corrosion of N80 steel in high temperature and high pressure formation water environment.

KEY WORDS: crevice corrosion; stress corrosion; thread; high temperature and pressure

在石油和天然气开采中，井下油管通常需要通过螺纹连接。然而，螺纹接头由于缝隙和应力的耦合作用可能产生严重的腐蚀损伤[1-4]。管道内部的腐蚀性介质会进入螺纹缝隙，由于缝内外化学环境的差异，可能形成缝隙腐蚀[5–6]。同时，螺纹接头承受油管自身质量所产生的拉应力，可能导致应力腐蚀开裂[7–8]。事实上，应力也会影响金属的局部腐蚀，可能增加局部腐蚀敏感性[9-10]。因此，缝隙和应力耦合作用会导致油管螺纹接头产生更为严重的腐蚀损伤。尽管对只有缝隙或应力单独存在的情况下的腐蚀行为已经进行了广泛的研究[11–14]，但对于缝隙和应力耦合作用下的腐蚀研究尚不多见。

Al-Jaroudi 等人[15]发现有机酸可以导致油管螺纹接头台肩面腐蚀。缝隙腐蚀是最危险的局部腐蚀之一，可在较短的时间内导致金属局部损伤[16–20]。一些研究表明，应力腐蚀开裂通常是由局部腐蚀缺陷引起的[21–23]。因此，缝隙腐蚀产生的局部缺陷可能是裂纹产生的根源，促进了应力腐蚀的发生。

文中设计了专门的实验装置，研究缝隙和拉应力耦合作用下 N80 钢在高温高压环境中的腐蚀行为，研究结果能为油井管材和螺纹选型提供参考。

1　实验装置设计

1.1　缝隙结构设计

样品表面缝隙结构如图 1 所示。试样上方依次放置 0.4 mm 厚 U 型垫片、1 mm 厚垫片，并用棉线对其进行固定。

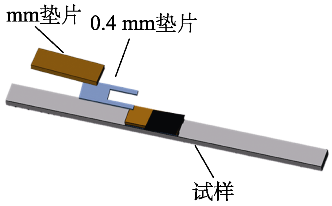

图 1　带缝隙试样结构
Fig.1　Schematic diagram of sample with a crevice

1.2　应力加载装置设计

采用二点弯的方式对样品施加应力，应力加载装置如图 2 所示。应力和缝隙耦合作用下的样品如图 3 所示。

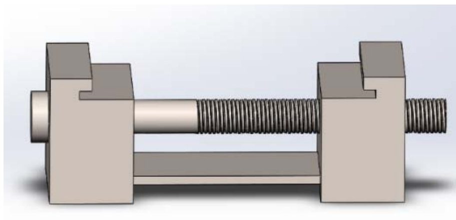

图 2　二点弯应力加载装置
Fig.2　Two-point bending stress loading device

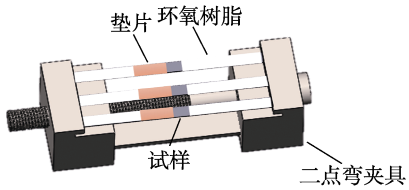

图 3　缝隙、应力耦合作用下的试样装置
Fig.3　Schematic diagram of sample under the combined crevice and stress

2　高温高压实验和方法

2.1　实验装置

在静态高温高压釜进行模拟实验，高压釜最高密封工作压力为 70 MPa，最高工作温度为 200 ℃，容积为 4.5 L。

2.2　实验材料和溶液

文中所选用材料为 N80 钢，其主要成分见表 1。实验溶液为 1.65% NaCl+700 mg/L HAc 的模拟地层水。向实验溶液中通入 CO_2 除氧，除氧后立即将其压入高温高压釜中。

表 1　N80 钢成分

Tab.1　Composition of N80 steel

Steel	C	Si	Mn	Fe
N80	1.95%	0.21%	1.68%	96.16%

2.3　表面分析

腐蚀产物膜的形貌和试样腐蚀后表面轮廓分别使用 ZEISSEV0 MA15 型扫描电镜和 Bruker ContourGT 型三维显微镜进行观察。由于试样会发生形变，对于产生弹性形变和塑性形变的试样，使用 3D 显微镜分别从 x 轴和 y 轴方向进行测量。

3　结果与分析

3.1　缝隙对 N80 钢腐蚀的影响

N80 钢在总压为 10 MPa、CO_2 分压为 3 MPa、40 ℃模拟地层水中，存在缝隙时，腐蚀 4 h 和 24 h 后，去除腐蚀产物膜前后的宏观形貌如图 4 所示。可以看出，腐蚀时间为 4 h 的试样去除腐蚀产物膜后，缝隙内发生明显腐蚀；腐蚀 24 h 的试样去除腐蚀产物膜后，缝隙内外均产生腐蚀，但缝隙内腐蚀程度更为严重。无缝时样品腐蚀 4 h 与有缝隙时样品腐蚀 4 h 后的微观形貌如图 5 所示。由图 5 可知，缝隙内存在大量腐蚀产物，缝隙内的腐蚀程度相比于缝外更为严重。N80 钢在腐蚀 4 h 和 24 h 后去除腐蚀产物膜的 3D 显微镜形貌分析如图 6 和图 7 所示。可以看出，腐蚀 4 h 后样品表面高度从缝隙外到缝隙内逐渐下

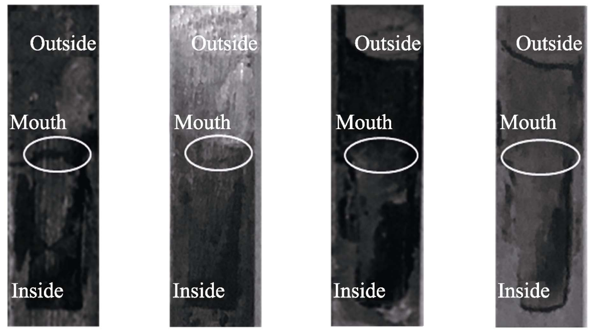

a 去膜前−4 h　b 去膜后−4 h　c 去膜前−24 h　d 去膜后−24 h

图 4　40 ℃、CO_2 分压 3 MPa、仅有缝隙条件下的宏观形貌

Fig.4　Macroscopic morphology of the sample with a crevice at 40 ℃ and 3 MPa CO_2: a) 4 h before film removal; b) 4 h after film removal; c) 24 h before film removal; d) 24 h after film removal

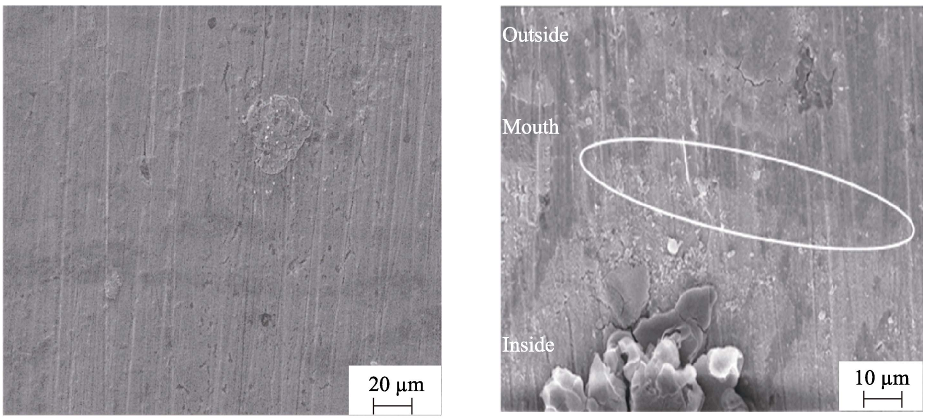

a 无缝隙　b 有缝隙

图 5　40 ℃、CO_2 分压 3 MPa、仅有缝隙与无缝隙条件下微观形貌对比

Fig.5　Microstructure of THE sample with/without a crevice at 40 ℃ and 3 MPa CO_2: a) without crevice; b) with crevice

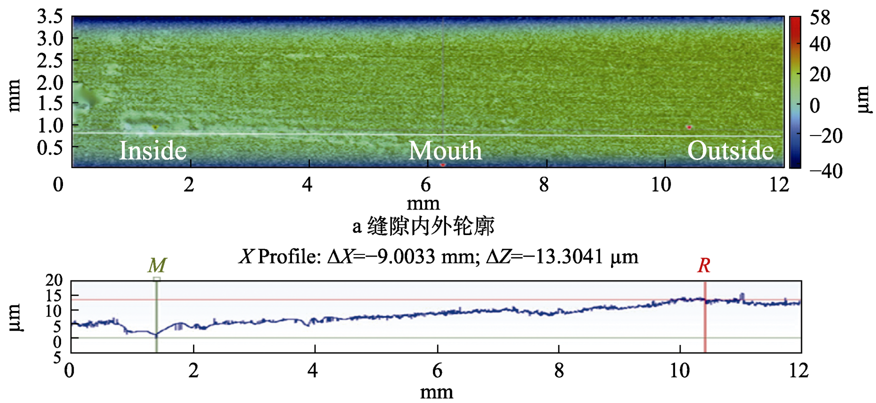

图 6　40 ℃、CO_2 分压 3 MPa、仅有缝隙条件下腐蚀 4 h 后 3D 显微镜结果

Fig.6　3D morphology of sample with a crevice at 40 ℃ and 3 MPa CO_2, exposed for 4 h: a) contour inside and outside the crevice; b) the x-axis contours

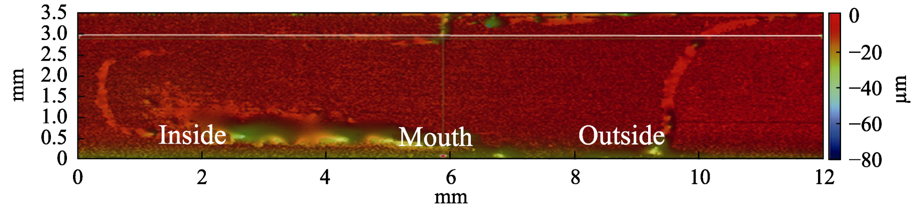

a 缝隙内外轮廓

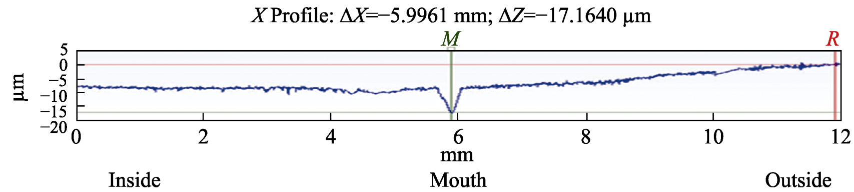

b x 轴向轮廓

图 7　40 ℃、CO_2 分压 3 MPa、仅有缝隙条件下腐蚀 24 h 后 3D 显微镜结果

Fig.7　3D morphology of sample with a crevice at 40 ℃ and 3 MPa CO_2, exposed for 24 h: a) contour inside and outside the crevice; b) the *x*-axis contours

降，这说明缝内金属比缝外腐蚀更为严重；腐蚀 24 h 后的试样在缝隙口处生成了 17.2 µm 的凹槽。

N80 钢在总压为 10 MPa、CO_2 分压为 3 MPa、70 ℃时，有缝隙时去除腐蚀产物膜前后的形貌如图 8 所示。由图 8 可知，相比于 40 ℃，缝隙口处产生了大量腐蚀产物。腐蚀 24 h 去除腐蚀产物膜后的 3D 显微镜形貌如图 9 所示。在腐蚀 24 h 后，在缝隙口处有 82.7 µm 的凹槽形成，约为 40 ℃时凹槽深度的 5 倍，这说明温度的升高加剧了缝隙腐蚀。

3.2　缝隙–应力耦合对 N80 钢腐蚀的影响

N80 钢在总压为 10 MPa、CO_2 分压为 3 MPa、40 ℃时，存在缝隙的试样分别在弹性变形和塑性变形下去除腐蚀产物膜前后的形貌如图 10 所示。可以发现，发生弹性变形的试样缝隙外表面几乎未产生腐蚀，缝隙内则发生严重腐蚀；发生塑性变形的试样则在缝隙内外均产生腐蚀。腐蚀 24 h 后的试样在缝隙口处发生严重腐蚀，去膜后，可以发现缝隙内腐蚀程度更为严重。

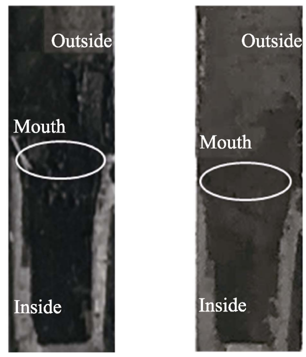

a 去膜前–24 h　b 去膜后–24 h

图 8　70 ℃、CO_2 分压 3 MPa、缝隙存在下宏观形貌

Fig.8　Macroscopic morphology of the sample with a crevice at 70 ℃ and 3 MPa CO_2: a) 24 h before film removal; b) 24 h after film removal

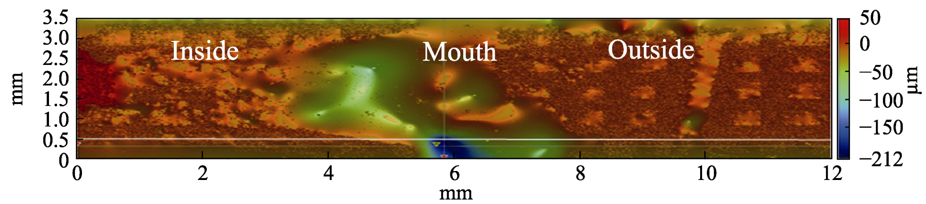

a 缝隙内外轮廓

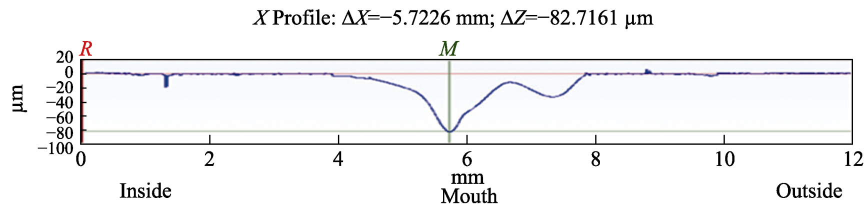

b x 轴向轮廓

图 9　70 ℃、CO_2 分压 3 MPa、缝隙存在下腐蚀 24 h 后 3D 显微镜结果

Fig.9　3D morphology of sample with a crevice at 70 ℃ and 3 MPa CO_2, exposed for 24 h: a) contour inside and outside the crevice; b) the X-axis contours

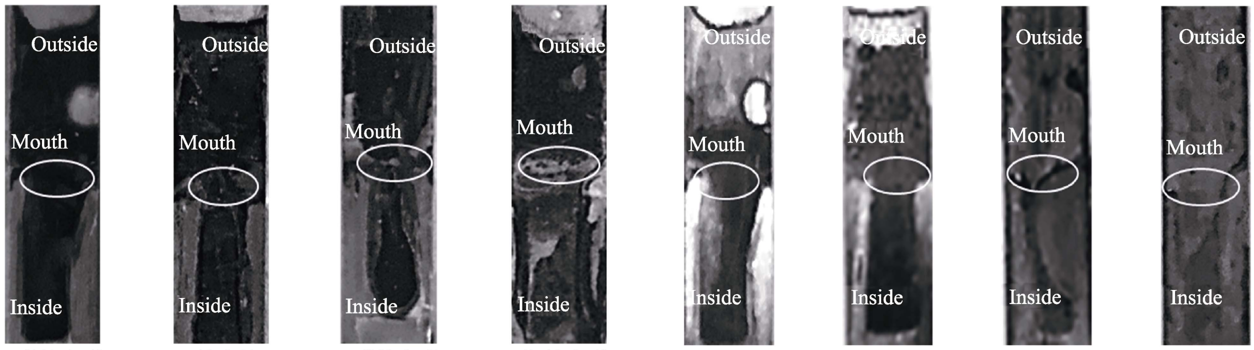

a 弹性变形 去膜前-4 h　b 性变性 去膜前s-4 h　c 弹性变形 去膜前-24 h　d 塑性变形 去膜后-24 h　e 弹性变形 去膜后-4 h　f 塑性变形 去膜后-4 h　g 弹性变形 去膜后-24 h　h 塑性变形 去膜后-24 h

图 10　40 ℃、CO_2 分压 3 MPa、缝隙和应力耦合条件下宏观形貌

Fig.10　Macroscopic morphology of the sample with a crevice and stress loading at 40 ℃ and 3 MPa CO_2: a)4 h-elastic deformation-before film removal; b)4 h- plastic deformation-before film removal; c)24 h- elastic deformation-before film removal; d)24 h- plastic deformation-before film removal; e)4 h- elastic deformation-after film removal; f)4 h- plastic deformation-after film removal; g)24 h- elastic deformation-after film removal; h)24 h- plastic deformation-after film removal

存在缝隙的试样去除腐蚀产物膜后的 3D 显微镜形貌如图 11—14 所示。可以看出，发生弹性变形时，缝隙内的腐蚀深度明显大于缝隙外，腐蚀 4 h 时和 24 h 的凹槽深度分别为 20.2 μm 和 35.3 μm。发生塑性变形时，腐蚀 4 h 时和 24 h 凹槽深度分别为 24.0 μm 和 41.3 μm。

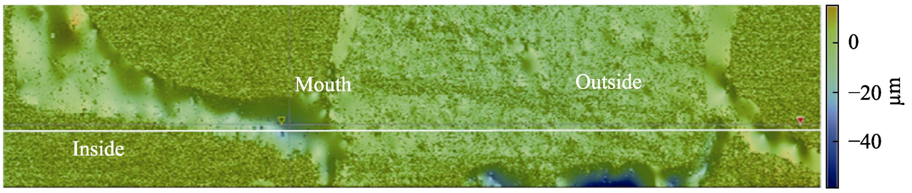

a 缝隙内外轮廓

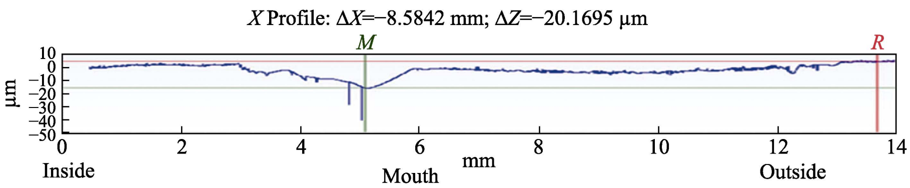

b x 轴向轮廓

图 11　40 ℃、CO_2 分压 3 MPa、缝隙和弹性变形耦合条件下腐蚀 4 h 后 3D 显微镜结果

Fig.11　3D morphology of the sample with a crevice and elastic deformation at 40 ℃ and 3 MPa CO_2, exposed for 4 h: a) contour inside and outside the crevice; b) X-axis contour

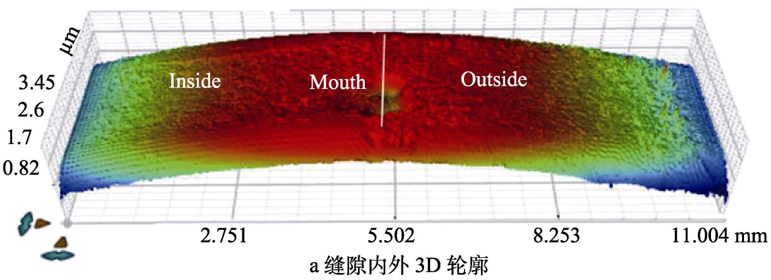

a 缝隙内外 3D 轮廓

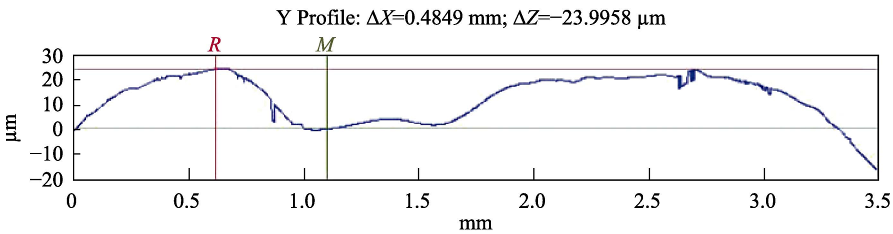

b y 轴向轮廓

图 12　40 ℃、CO_2 分压 3 MPa、缝隙和塑性变形耦合条件下下腐蚀 4 h 后 3D 显微镜结果

Fig.12　3D morphology of the sample with a crevice and plastic deformation at 40 ℃ and 3 MPa CO_2, exposed for 4 h: a) 3D contour inside and outside the crack; b) *y*-axis contour

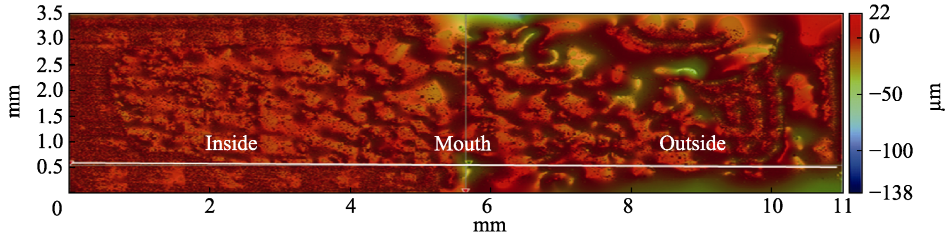

a 缝隙内外轮廓

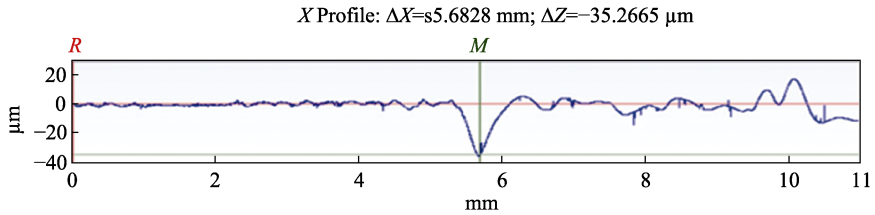

b *x* 轴向轮廓

图 13　40 ℃、CO_2 分压 3 MPa、缝隙和弹性变形耦合条件下腐蚀 24 h 后 3D 显微镜结果

Fig.13　3D morphology of sample with a crevice and elastic deformation at 40 ℃ and 3 MPa CO_2, exposed for 24 h: a) contour inside and outside the crevice; b) Y-axis contour

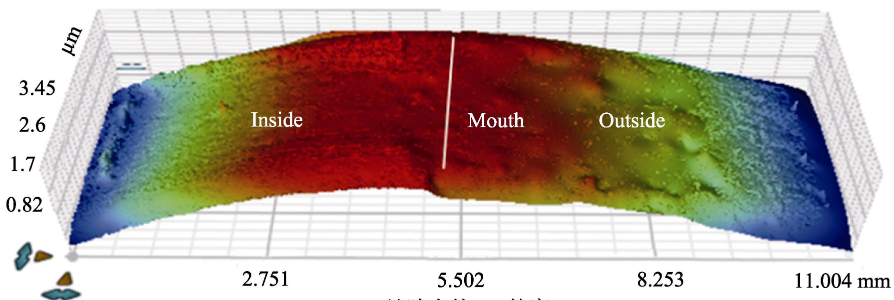

a 缝隙内外 3D 轮廓

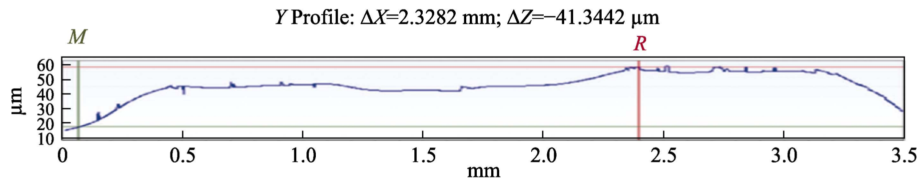

b y 轴向轮廓

图 14　40 ℃，CO_2 分压 3 MPa，缝隙和塑性变形耦合条件下腐蚀 24 h 后 3D 显微镜结果：(a)，(b)

Fig.14　3D morphology of sample with a crevice and plastic deformation at 40 ℃ and 3 MPa CO_2, exposed for 24 h: a) 3D contour inside and outside the crevice; b) Y-axis contour

N80 钢在总压为 10 MPa、CO_2 分压为 3 MPa、70 ℃时，缝隙试样在弹性变形和塑性变形耦合下去除腐蚀产物膜前后的形貌如图 15 所示。腐蚀 24 h 后的试样在缝隙口处存在严重腐蚀。去膜后，缝内及缝隙口处腐蚀情况较缝隙外较远位置更为严重。有缝隙试样去除腐蚀产物膜后的 3D 显微镜形貌如图 16 和 17 所示。可以看出，在弹性变形和塑性耦合情况下，缝隙试样的凹槽深度分别为 143.7 μm 和 243.9 μm。这主要是由于应力的施加会加剧 N80 钢的缝隙腐蚀，导致形成更深的腐蚀凹槽，这反过来又会导致应力的进一步集中，产生更高的应力腐蚀开裂敏感性。因此，缝隙和应力对 N80 钢在高温高压地层水环境中的腐蚀具有协同作用。

根据 3D 显微镜结果，N80 钢在不同腐蚀环境下的局部腐蚀速率见表 2，缝隙和应力耦合作用下缝隙口处凹槽的深度较仅有缝隙存在条件下的深度更深，且深度随着温度的升高而逐渐增大。

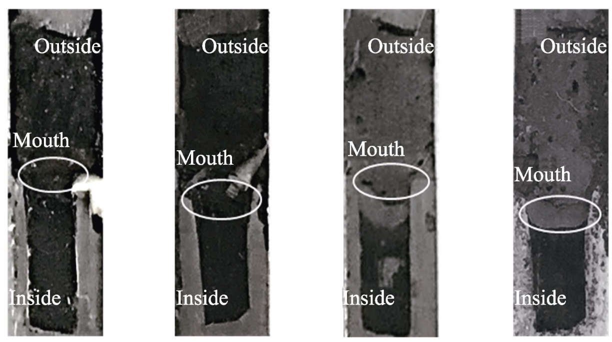

a 去膜前-弹性变形　b 去膜前-塑性变形　c 去膜后-弹性变形　d 去膜后-塑性变形

图 15　70 ℃、CO_2 分压 3 MPa、缝隙和应力耦合条件下宏观形貌

Fig.15　Macroscopic morphology of the sample with a crevice and stress loading at 70 ℃ and 3 MPa CO_2: a) elastic deformation-before film removal; b) plastic deformation-before film removal; c) elastic deformation-after film removal; d) plastic deformation-after film removal

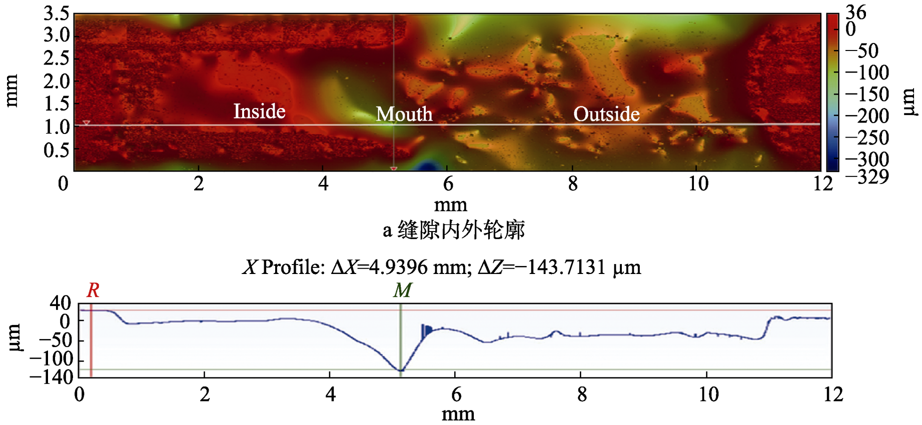

b x 轴向轮廓

图 16 70 ℃、CO_2 分压 3 MPa、缝隙和弹性变形耦合条件下腐蚀 24 h 后 3D 显微镜结果

Fig.16 3D morphology of sample with a crevice and elastic deformation at 70 ℃ and 3 MPa CO_2, exposed for 24 h: a) contour inside and outside the crack; b) x-axis contour

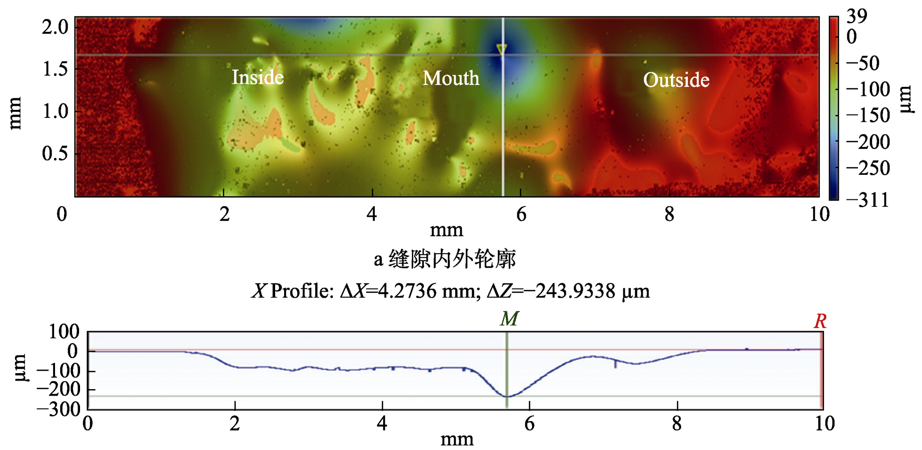

b y 轴向轮廓

图 17 70 ℃、CO_2 分压 3 MPa、缝隙和塑性变形耦合条件下腐蚀 24 h 后 3D 显微镜结果：(a)，(b)

Fig.17 3D morphology of sample with a crevice and plastic deformation at 70 ℃ and 3 MPa CO_2, exposed for 24 h: a) contour inside and outside the crevice; b) *y*-axis contour

表 2 N80 钢在不同腐蚀环境下的局部腐蚀速率

Tab.2 Localized corrosion rate of N80 steel in different corrosion environments

腐蚀环境	40 ℃		70 ℃	
	24 h 局部腐蚀深度/μm	局部腐蚀速率/$(mm \cdot a^{-1})$	24 h 局部腐蚀深度/μm	局部腐蚀速率/$(mm \cdot a^{-1})$
缝隙腐蚀	17.2	6.3	82.7	30.2
缝隙腐蚀、弹性变形耦合	35.3	12.9	143.7	52.4
缝隙腐蚀、塑性变形耦合	41.3	15.1	243.9	89.0

4 结语

1）有无缝隙时的表面微观形貌存在显著差异：缝内存在大量腐蚀产物，相反缝外几乎未见腐蚀产物，缝外腐蚀程度相比缝内腐蚀程度较轻。试样在缝隙口处产生凹槽，且凹槽深度随着时间和温度的升高而增加。70 ℃时凹槽处腐蚀深度达到 82.7 μm，约为 40 ℃时凹槽处腐蚀深度的 5 倍。

2）在缝隙和应力耦合作用下使得缝隙口处凹槽的深度增加，且随着腐蚀时间和温度的增加，深度也逐渐增大，且塑性变形相比于弹性变形时会产生更大的凹槽深度。70 ℃时，弹性变形的试样缝隙口处凹槽深度约为 143.7 μm，是单独缝隙腐蚀深度的 1.73 倍；塑性变形的试样缝隙口处凹槽深度约为 243.9 μm，是单独缝隙腐蚀深度的 3 倍。这表明应力的施加会加剧 N80 钢的缝隙腐蚀，导致形成更深的腐蚀凹槽，这反过来又会导致应力的进一步集中，产生更高的应力腐蚀开裂敏感性。因此，缝隙和应力对 N80 钢在高温高压地层水环境中的腐蚀具有协同作用。

参考文献：

[1] HAY M G. Fitness-for-Purpose Material Testing for Sour Gas Service—An Overview[J]. Corrosion, 2001, 57(3): 236-252.

[2] VAN GELDER K, ERLINGS J G, DAMEN J W, et al. The Stress Corrosion Cracking of Duplex Stainless Steel in $H_2S/CO_2/Cl^-$ Environments[J]. Corrosion Science, 1987, 27(10): 1271-1279.

[3] ALBARRAN J L, MARTINEZ L A, LOPEZ H F, et al. Effect of Heat Treatment on the Stress Corrosion Resistance of a Microalloyed Pipeline Steel[J]. Corrosion Science, 1999, 41(6): 1037-1049.

[4] 张光普, 陈继明, 张效羽, 等. 我国油田套管损坏的原因探讨[J]. 石油钻采工艺, 1996, 18(5): 7-12.
ZHANG Guang-pu, CHEN Ji-ming, ZHANG Xiao-Yu, et al. Discussion on the Causes of Casing Damage in Chinese oil Fields[J]. Oil Drilling & Production Technology, 1996, 18(5): 7-12.

[5] ZHU S D, WEI J F, BAI Z Q, et al. Failure Analysis of P110 Tubing String in the Ultra-deep Oil Well[J]. Engineering Failure Analysis, 2011, 18(3): 950-962.

[6] SAMPANTHAR J T, XIAO H, DOU J, et al. A Novel Oxidative Desulfurization Process to Remove Refractory Sulfur Compounds from Diesel Fuel[J]. Applied Catalysis B Environmental, 2006, 63(1): 85-93.

[7] WU T, XU J, SUN C, et al. Microbiological Corrosion of Pipeline Steel under Yield Stress in Soil Environment[J]. Corrosion Science, 2014, 88: 291-305.

[8] ZHU M, DU C, LI X, et al. Effect of AC on Stress Corrosion Cracking Behavior and Mechanism of X80 Pipeline Steel in Carbonate/Bicarbonate Solution[J]. Corrosion Science, 2014, 87: 224-232.

[9] YAN M, SUN C, XU J, et al. Stress Corrosion of Pipeline Steel under Occluded Coating Disbondment in a Red Soil Environment[J]. Corrosion Science, 2015, 93: 27-38.

[10] ZHANG G, CHENG Y F. Micro-electrochemical Characterization and Mott-schottky Analysis of Corrosion of Welded X70 Pipeline Steel in Carbonate/Bicarbonate Solution[J]. Electrochimica Acta, 2009, 55(1): 316-324.

[11] LU B T, CHEN Z K, LUO J, et al. Pitting and Stress Corrosion Cracking Behavior in Welded Austenitic Stainless Steel[J]. Electrochimica Acta, 2005, 50(6): 1391-1403.

[12] YANG H Q, ZHANG Q, TU S S, et al. Effects of Inhomogeneous Elastic Stress on Corrosion Behaviour of Q235 Steel in 3.5% NaCl Solution Using a Novel Multi-channel Electrode Technique[J]. Corrosion Science, 2016, 110: 1-14.

[13] GUAN L, ZHANG B, YONG X P, et al. Effects of Cyclic Stress on the Metastable Pitting Characteristic for 304 Stainless Steel under Potentiostatic Polarization[J]. Corrosion Science, 2015, 93(93): 80-89.

[14] LIU Z, LI X, DU C, et al. Stress Corrosion Cracking Behavior of X70 Pipe Steel in an Acidic Soil Environment[J]. Corrosion Science, 2008, 50(8): 2251-2257.

[15] AL-JAROUDI S S, UL-HAMID A, MOHAMMED A. Premature Failure of Tubing Used in Sweet Extra Arab Light Grade Crude Oil Production Well[J]. Engineering Failure Analysis, 2015, 47: 178-198.

[16] YANG Y Z, JIANG Y M, LI J. In Situ Investigation of Crevice Corrosion on UNS S32101 Duplex Stainless Steel in Sodium Chloride Solution[J]. Corrosion science, 2013, 76: 163-169.

[17] CAI B P, LIU Y H, TIAN X J, et al. An Experimental Study of Crevice Corrosion Behaviour of 316L Stainless Steel in Artificial Seawater[J]. Corrosion Science, 2010, 52(10): 3235-3242.

[18] NAGARAJAN S, RAJENDRAN N. Crevice Corrosion Behaviour of Superaustenitic Stainless Steels: Dynamic Electrochemical Impedance Spectroscopy and Atomic Force Microscopy Studies[J]. Corrosion Science, 2009, 51(2): 217-224.

[19] TORKKELI J, SAUKKONEN T, HANNINEN H. Effect of MnS Inclusion Dissolution on Carbon Steel Stress Corrosion Cracking in Fuel-grade Ethanol[J]. Corrosion Science, 2015, 96: 14-22.

[20] LUO L H, HUANG Y H, XUAN F Z. Pitting Corrosion and Stress Corrosion Cracking around Heat Affected Zone in Welded Joint of CrNiMoV Rotor Steel in Chloridized High Temperature Water[J]. Procedia Engineering, 2015, 130: 1190-1198.

[21] YOO S C, CHOI K J, KIM T, et al. Microstructural Evolution and Stress-corrosion-cracking Behavior of Thermally Aged Ni-Cr-Fe Alloy[J]. Corrosion Science, 2016, 111: 39-51.